Functional dissection of the multi-domain di-heme cytochrome c(550) from Thermus thermophilus.

Sylvain Robin, Marzia Arese, Elena Forte, Paolo Sarti, Olga Kolaj-Robin, Alessandro Giuffrè, Tewfik Soulimane

OPEN ACCESS Freely available online

PLOS ONE

Functional Dissection of the Multi-Domain Di-Heme Cytochrome c_{550} from *Thermus thermophilus*

Sylvain Robin[1], Marzia Arese[2], Elena Forte[2], Paolo Sarti[2,3], Olga Kolaj-Robin[1], Alessandro Giuffrè[3]*, Tewfik Soulimane[1]*

1 Chemical and Environmental Science Department, Materials and Surface Science Institute, University of Limerick, Limerick, Ireland, **2** Department of Biochemical Sciences and Istituto Pasteur – Fondazione Cenci Bolognetti, Sapienza University of Rome, Rome, Italy, **3** Consiglio Nazionale delle Ricerche Istituto di Biologia e Patologia Molecolari, Rome, Italy

Abstract

In bacteria, oxidation of sulfite to sulfate, the most common strategy for sulfite detoxification, is mainly accomplished by the molybdenum-containing sulfite:acceptor oxidoreductases (SORs). Bacterial SORs are very diverse proteins; they can exist as monomers or homodimers of their core subunit, as well as heterodimers with an additional cytochrome *c* subunit. We have previously described the homodimeric SOR from *Thermus thermophilus HB8* (SOR_{TTHB8}), identified its physiological electron acceptor, cytochrome c_{550}, and demonstrated the key role of the latter in coupling sulfite oxidation to aerobic respiration. Herein, the role of this di-heme cytochrome *c* was further investigated. The cytochrome was shown to be composed of two conformationally independent domains, each containing one heme moiety. Each domain was separately cloned, expressed in *E. coli* and purified to homogeneity. Stopped-flow experiments showed that: i) the N-terminal domain is the only one accepting electrons from SOR_{TTHB8}; ii) the N- and C-terminal domains are in rapid redox equilibrium and iii) both domains are able to transfer electrons further to cytochrome c_{552}, the physiological substrate of the ba_3 and caa_3 terminal oxidases. These findings show that cytochrome c_{550} functions as a electron shuttle, without working as an electron wire with one heme acting as the electron entry and the other as the electron exit site. Although contribution of the cytochrome c_{550} C-terminal domain to *T. thermophilus* sulfur respiration seems to be dispensable, we suggest that di-heme composition of the cytochrome physiologically enables storage of the two electrons generated from sulfite oxidation, thereof ensuring efficient contribution of sulfite detoxification to the respiratory chain-mediated energy generation.

Citation: Robin S, Arese M, Forte E, Sarti P, Kolaj-Robin O, et al. (2013) Functional Dissection of the Multi-Domain Di-Heme Cytochrome c_{550} from *Thermus thermophilus*. PLoS ONE 8(1): e55129. doi:10.1371/journal.pone.0055129

Editor: Ligia M. Saraiva, Instituto de Tecnologia Quimica e Biologica, Portugal

Received November 14, 2012; **Accepted** December 18, 2012; **Published** January 31, 2013

Funding: Work partially supported by Science Foundation Ireland (BICF685) to TF and Ministero dell'Istruzione, dell'Università e della Ricerca of Italy (FIRB RBFR08F41U_001 to AG and FIRB RBIN06E9Z8 to PS). The funders had no role in study design, data collection and analysis, decision to publish, or preparation of the manuscript.

Competing Interests: The authors have declared that no competing interests exist.

* E-mail: alessandro.giuffre@uniroma1.it; tewfik.soulimane@ul.ie

Introduction

In addition to its natural occurrence in the environment, sulfite is an extremely important intermediary in sulfur metabolism, arising from a variety of reactions both in prokaryotes and eukaryotes [1–3]. The nucleophilicity and strong reducing capacity of sulfite account for its high toxicity. In the cell it can react with disulfide bonds causing protein inactivation and DNA damage. Although some microorganisms use sulfite as the sole electron/energy source [4,5], accumulation of sulfite in the cell generally leads to massive damage, so that both prokaryotic and eukaryotic cells require efficient sulfite detoxification systems.

The most common strategy for sulfite detoxification in *Bacteria* and *Archaea* involves oxidation to sulfate, accomplished either directly or indirectly *via* the adenosine 5′-phosphosulfate reductase pathway [2,6]. Molybdenum-containing sulfite:acceptor oxidoreductases (SORs) catalyze the direct oxidation of sulfite to sulfate. They have been identified in mammals [7], birds [8], plants [9] and prokaryotes [10]. Two types of SORs have been identified to date: i) the sulfite oxidases (EC 1.8.3.1) that are able to utilize O_2 as a direct electron acceptor, but also ferricyanide and sometimes cytochrome *c*, and ii) the sulfite dehydrogenases (EC 1.8.2.1) unable to transfer electrons to O_2. The first bacterial SOR was discovered almost half a century ago [11]. Although, since then, SORs have been shown to be widely distributed among bacteria, their exact physiological role is still elusive.

Compared to the vertebrate and plant enzymes, bacterial SORs are structurally much more diverse. The protein core consists of a molybdenum binding site and a dimerization domain. The enzymes can exist as monomers or homodimers of the core structure, as well as heterodimers with an additional cytochrome *c* subunit [10,12–16]. The SORs containing both the molybdenum cofactor and the additional cytochrome *c* subunit have been classified as Group 1 SORs, while members of the Group 2 contain only the molybdenum cofactor and are called 'atypical' SORs [17]. The name 'atypical' arises from the fact that most of these enzymes, if not all, cannot efficiently use horse heart cytochrome *c* as substrate and display higher activities when assayed with the artificial electron acceptor ferricyanide. To date, Group 1 includes only the cytochrome *c*-containing SOR isolated from *Starkeya novella* [10]. The SOR from *Campylobacter jejuni*, though originally defined as a two-subunit protein acting similarly to the *S. novella* enzyme, likely belongs to Group 2 SORs, as the

molybdenum- and the heme-containing subunits do not co-purify [18]. Similarly, all the other bacterial SORs so far described fall into Group 2 [12–16], thus calling for a revision of the term 'atypical'.

With the exception of the enzyme from *Deinococcus radiodurans*, all characterized SORs were interestingly found to be encoded upstream their putative physiological electron acceptors (*c*-type cytochromes or other redox proteins [19]). Consistently, the genes coding for the *c*-type cytochromes identified as electron acceptors for SORs from *S. novella* [10], *C. jejuni* [18], *Sinorhizobium meliloti* [20] and *Thermus thermophilus* [16] were all found downstream the relative SOR-encoding gene. These *c*-type cytochromes are also very diverse. They differ in size and heme content and this is an additional feature contributing to the complexity of SORs.

Several attempts have been made to elucidate how SOR-mediated sulfite oxidation is integrated in cell metabolism. It is postulated that Group 1 SORs are directly linked to the respiratory chain *via* their natural electron acceptor cytochromes [20]. In *S. novella*, cytochrome c_{550} [10] was tentatively suggested to enable the association between sulfite oxidation and aerobic respiration, based on the notion that cytochromes *c* are natural substrates for cytochrome *c* oxidases [20]; the hypothesis however, remains to be tested as yet. Similarly, in *C. jejuni* electrons from sulfite oxidation were proposed to enter the respiratory chain downstream the bc_1 complex *via* the natural substrate of *cb* oxidase [18]. Although such a scenario seems plausible, also in this case the exact electron transfer pathway and the redox proteins involved have not been identified. Only cell extracts, and not purified proteins, were used in these experiments and, indeed, one cannot exclude the involvement of additional, unidentified electron shuttles.

Recently, the connection to the respiratory chain was demonstrated for Group 2 SORs from *S. meliloti* [20] and *T. thermophilus* [16], whose natural electron acceptors (cytochrome *c* Smc04048 and cytochrome c_{550}, respectively) have been identified. In the former study [20], however, experiments were performed using isolated cell membranes and the association of the electron acceptor of SorT, cytochrome *c* Smc04048, with cytochrome oxidases remains to be proven. On the contrary, in the latter study on *T. thermophilus* the complete electron transfer pathway linking sulfite oxidation to oxygen reduction was unveiled [16]. Accordingly, the electrons generated upon sulfite oxidation by SOR_{TTHB8} are transferred to the natural electron acceptor of the enzyme, cytochrome c_{550}, and from here to cytochrome c_{552}, the physiological electron donor of the two terminal cytochrome *c* oxidases, ba_3 and caa_3.

Here, the role of *T. thermophilus* cytochrome c_{550} in coupling sulfite oxidation to cell respiration has been further investigated.

Materials and Methods

Purification of Cytochrome c_{552} and the Cytochrome c Oxidases ba_3 and caa_3

Native ba_3- and caa_3-type cytochrome *c* oxidases were isolated from *T. thermophilus* HB8 cells according to previously published procedures [21,22]. Native cytochrome c_{552} was purified according to Soulimane and co-authors [23]. Purified proteins were concentrated by ultrafiltration, fast frozen in liquid nitrogen and stored at $-80^{\circ}C$.

Expression and Purification of SOR_{TTHB8} and Cytochrome c_{550}

Expression and purification of the proteins were conducted as described previously [16].

Determination of Cytochromes and Cytochrome Oxidases Concentration

UV/vis absorption spectra were recorded with a Perkin Elmer Lambda 5 spectrophotometer. Concentration of the proteins was obtained from the dithionite reduced-minus oxidized spectra using the following extinction coefficients: $\varepsilon = 18000\ M^{-1}\ cm^{-1}$ ($\lambda = 550$ nm) for cytochrome c_{550}; $\varepsilon = 21000\ M^{-1}\ cm^{-1}$ ($\lambda = 552$ nm) for cyt c_{552}; $\varepsilon = 6300\ M^{-1}\ cm^{-1}$ ($\lambda = 613$ nm) for ba_3 oxidase and $\varepsilon = 24000\ M^{-1}\ cm^{-1}$ ($\lambda = 604$ nm) for caa_3 oxidase. The concentration of SOR_{TTHB8} was determined using $\varepsilon = 67350\ M^{-1}\ cm^{-1}$ ($\lambda = 280$ nm).

Limited Proteolysis

Cytochrome c_{550} was subjected to limited proteolysis by trypsin (Sigma-Aldrich) for 90 minutes at 37°C in 25 mM Tris-HCl pH 8.2, at a cytochrome:trypsin mass ratio of 100:1. To separate the proteolytic products, the reaction mixture was diluted with water and loaded on a Fractogel® TMAE 650(S) column (Merck, Germany) equilibrated with 5 mM Tris-HCl pH 8.2. The flowthrough was collected, the column washed with the equilibration buffer and finally bound proteins were eluted with the same buffer containing 150 mM NaCl.

Construction of the Cytochrome c_{550} Domains Expression Plasmids

The sequence encoding the mature N-terminal domain of cytochrome c_{550} (c_{550}[N]) was amplified from *T. thermophilus* HB8 genomic DNA by PCR using the primers 5′–ATCTGACCATGGCTCAGACCACCCTCCCCGAG–3′, containing *Nco*I restriction site (underlined), and 5′–CAGTGACTCGAGTCAGGCAGGGGTCTCCTGGGCTG–3′, containing *Xho*I restriction site (underlined). Similarly, the sequence encoding the mature C-terminal domain of cytochrome c_{550} (c_{550}[C]) was amplified using the primers 5′–ATCTGACCATGGCTCCCAAAACGGGAGCCCAGGTCTAC–3′, containing *Nco*I restriction site (underlined), and 5′–CAGTGACTCGAGTCATGGCAGTTTGAGGCCTTGGCGGAG–3′, containing *Xho*I restriction site (underlined). The products were *Nco*I and *Xho*I cloned into the expression vector pET22b+ (Invitrogen) to yield the pET22bC550N and pET22bC550C vectors. These constructs permit the expression of the recombinant domains in *E. coli*, fused to the *pelB* leader sequence for an optimal translocation to the periplasmic space.

Expression and Purification of the Recombinant Cytochrome c_{550} N-terminal Domain (c_{550}[N])

The BL21(DE3) *E. coli* strain was co-transformed with the pET22bC550N and pEC86 vectors [24], the latter containing the cytochrome maturation gene cluster necessary for the production of cytochrome *c* in *E. coli* under aerobic conditions [25]. The recombinant c_{550}[N] was produced by growing the cells in LB medium containing ampicillin (100 μg/ml) and chloramphenicol (34 μg/ml) at 37°C for 24 h under shaking, and without protein expression inducers. Periplasmic proteins were prepared from fresh biomass. Cells were washed in PBS buffer (20 mM phosphate, 135 mM NaCl, 1 mM KCl, pH 7.4) and spun down at $8000 \times g$ for 20 min at 4°C. The pellet was resuspended in 100 mM Tris-HCl pH 8 buffer containing 0.75 M sucrose. Osmotic shock was induced by slowly adding 2 volumes of ice chilled 1 mM EDTA. Following 10 min incubation at room temperature, spheroplasts were prepared by incubation with 1 mg/ml lysozyme for 45 min at room temperature under gentle shaking. Following the addition of 25 mM $MgCl_2$, and 50 μg/ml

DNaseI to reduce the viscosity of the extract, intact spheroplasts were removed by centrifugation at 8000×*g* for 10 min at 4°C. The supernatant containing the recombinant domain was extensively dialyzed against 5 mM Tris-HCl pH 8.0 and then loaded on a Fractogel® TMAE 650(S) (Merck, Germany) column equilibrated at 4°C with the same buffer. The protein was eluted with a gradient of NaCl (0–250 mM) and the fractions containing the protein were pooled, concentrated and desalted using a PD10 column (GE Healthcare, Germany) equilibrated with 5 mM Tris-HCl pH 8.0. The eluate was then loaded on a CaptoQ XL anion exchange column (GE Healthcare, Germany) equilibrated with the same buffer and eluted with a gradient of NaCl (0–150 mM). Fractions containing the domain were pooled, concentrated and finally purified by gel filtration on a Superdex 75 column (GE Healthcare, Germany) at 4°C with 5 mM Tris-HCl pH 8.0 buffer containing 150 mM NaCl. The isolated protein was concentrated by ultrafiltration, fast frozen in liquid nitrogen and stored at −80°C.

Expression and Purification of the Recombinant Cytochrome c_{550} C-terminal Domain (c_{550}[C])

The C-terminal domain was expressed and initially extracted as described above for the N-terminal domain. The supernatant containing the c_{550}[C] domain was extensively dialyzed against 5 mM Tris-acetate buffer pH 6.0 and then loaded on a CM Sepharose® (Merck, Germany) column equilibrated at 4°C with the same buffer. The protein was eluted with a gradient of NaCl (0–250 mM) and the fractions containing the protein were pooled, concentrated and finally purified by gel filtration on a Superdex 75 column (GE Healthcare, Germany) at 4°C with 5 mM Tris-HCl pH 8.0 buffer containing 150 mM NaCl. The last step was repeated twice. The isolated protein was concentrated by ultrafiltration, fast frozen in liquid nitrogen and stored at −80°C.

Analytical Size Exclusion Chromatography

Analysis of the association of cytochrome c_{550} domains was carried out by analytical size exclusion chromatography (SEC). 1.3×10^{-8} moles of each domain were incubated for one hour at room temperature in 10 mM Tris-HCl, 50 mM NaCl, pH 8.0 before injection on a Superdex S75 10/30 column at a flow-rate of 0.5 ml/min. Elution profiles were recorded at 280 nm. The cytochrome full-length was analysed in a similar way.

Electron Transfer activity

Stopped-flow experiments were carried out with a thermostated instrument (DX.17 MV, Applied Photophysics, Leatherhead, UK), equipped with a 1-cm pathlength observation chamber. Reactions were investigated by monitoring the absorption changes at selected wavelengths. When necessary, ionic strength was adjusted by addition of KCl and the buffer was degassed with vacuum/N_2 cycles. Data were analyzed using the software MATLAB (The Mathworks, South Natick, MA).

Reduction by SOR_{TTHB8} of the cytochrome c_{550} and its domains was investigated anaerobically at 45°C in 100 mM Tris-HCl pH 8.0 buffer containing 0.1 mM EDTA. To prevent inhibition of SOR_{TTHB8} resulting from prolonged incubation of the enzyme with a large excess of sulfite, in these experiments the stopped-flow instrument was used in the sequential mixing mode. Typically, 2 µM SOR_{TTHB8} was pre-mixed with 4 mM sulfite and after 500 ms further mixed with increasing amounts of oxidized cytochrome c_{550}, c_{550}[N], c_{550}[C] or a 1:1 mixture of the two domains. The reduction of the cytochrome or its domains was monitored at 418 nm or, in the case of a too high signal in the Soret region, at 555 nm. The turnover rates (TN) of reduction of cytochrome c_{550} and its domains were calculated by dividing the concentration (expressed in µM) of the c_{550} sample reduced at $t = t_{½}$ by the half time of the reaction and the concentration of SOR_{TTHB8} in the experiment (typically 0.5 µM after mixing).

The kinetics of electron transfer between ascorbate-reduced cyt c_{550} (or its domains) and cyt c_{552} was assayed anaerobically at 4°C. This low temperature was chosen to slow-down and thus better resolve in time the reactions. Experiments were carried out in 5 mM Bis-Tris pH 7.0 buffer under non-pseudo-first order conditions, i.e., at comparable concentrations of the two proteins. Observed rate constants (k_{obs}) were therefore obtained by fitting the experimental time courses to the equations described in [26] for the analysis of bimolecular reactions assayed under second-order conditions.

The oxidation of cytochrome c_{550} and its domains by ba_3- or caa_3-oxidase was assayed at 25°C in 5 mM Bis-Tris pH 7.0 buffer complemented with 0.1% *n*-Dodecyl-β-D-maltoside. Approximately 1.5 µM c_{550}, c_{550}[C], c_{550}[N] or a 1:1 mixture of the two domains was pre-reduced with 300 µM ascorbate and stopped-flow mixed with air-equilibrated buffer containing either ba_3-(200 nM) or caa_3-oxidase (200 nM). The reaction was followed at 418 nm.

Results

The Cytochrome c_{550} is Composed of Two Conformationally Independent Domains

The recently identified periplasmic di-heme cytochrome c_{550} [16] as a whole shows poor similarity to known proteins. However, when analyzed separately, its N-terminal domain sequence containing one heme binding site presents a high homology to the subunit B of SOR from *C. jejuni* [18], whereas the C-terminal domain, containing the other heme binding site, exhibits a high sequence identity with c_{552} from *T. thermophilus* HB8. This led to the hypothesis that cytochrome c_{550} is likely organized in two distinct domains, each one possibly presenting an independent fold and a heme cofactor, with distinct roles in mediating electron transfer between SOR_{TTHB8} and the respiratory chain, through cytochrome c_{552} [16].

Consistently, according to the DomPred server [27] cytochrome c_{550} consists of two domains, with a predicted boundary at residue 107 and a proline rich region (91–106 aa) likely representing a flexible inter-domain linker [28] (Figure 1A). While globular proteins, due to their native rigid structure, are typically resistant to proteolysis under physiological conditions, flexible inter-domain linkers can be substrates for proteases. This makes the limited proteolysis approach suitable to confirm the multi-domain organization of a protein [29]. Based on this notion, cytochrome c_{550} was subjected to limited proteolysis using trypsin. Overall, the cytochrome presents 19 putative cleavage sites for this protease (Figure 1A). Among these sites, the one in position K105 is of particular interest, as it is located within the predicted linker, being therefore potentially more accessible to the protease. On this basis, limited proteolysis of the recombinant cytochrome c_{550} is expected to yield the N- and C-terminal domains as the major cleavage products.

As c_{550}[N] and c_{550}[C] have significantly different calculated isoelectric points (5 and 7.97, respectively), the two domains are expected to have opposite net charges at pH 7, being easily separable by ion exchange (IEX) chromatography. The products of the limited proteolysis of cytochrome c_{550} were therefore directly subjected to analytical IEX chromatography using the basic anionic exchanger Fractogel® EMD TMAE (S) and subsequently

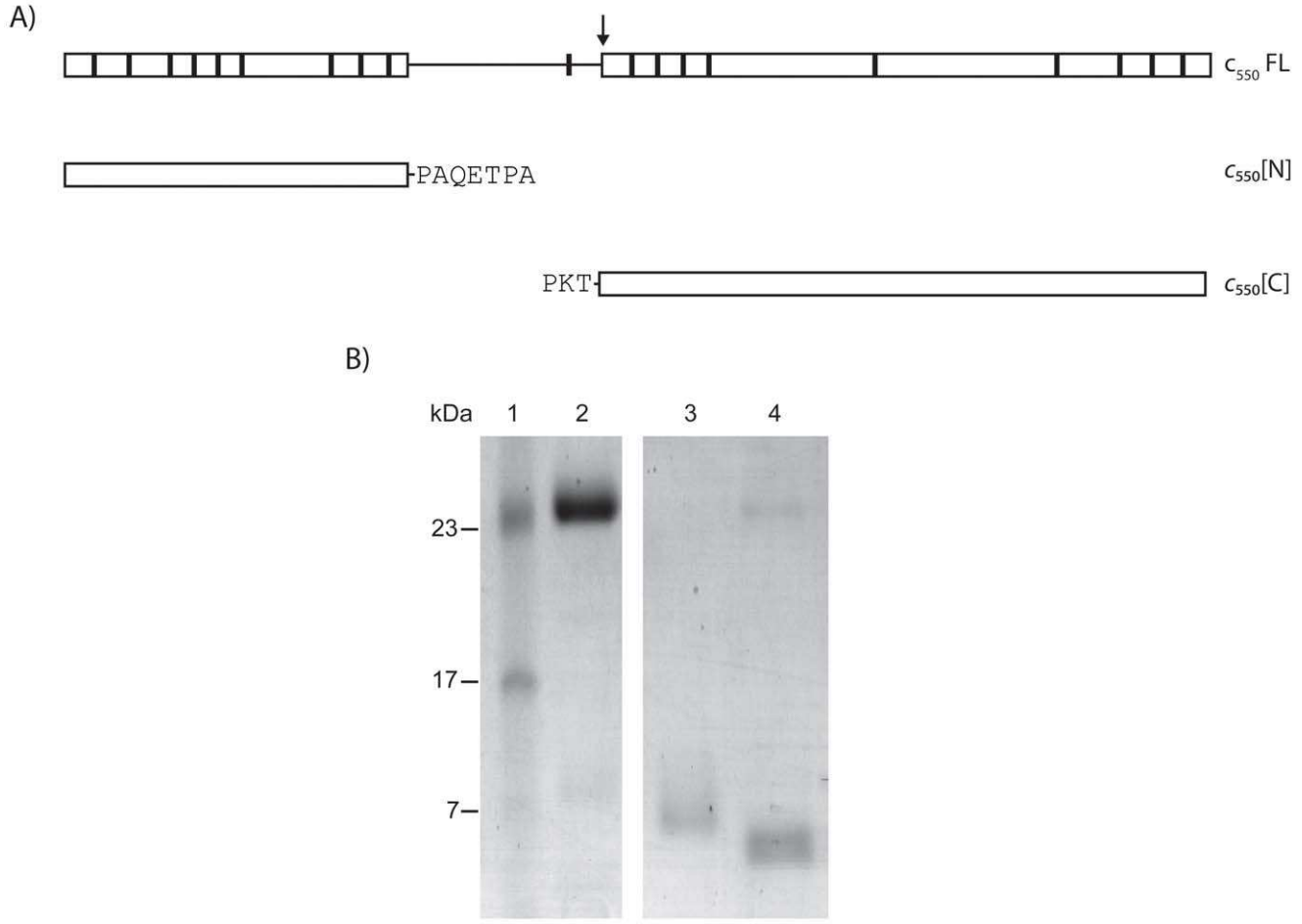

Figure 1. Domains of *T. thermophilus* cytochrome c_{550}. The schematic representation of the full-length cytochrome c_{550} (FL) with predicted trypsin cleavage sites (vertical lines) and the cloned c_{550}[N] and c_{550}[C] domains is shown in panel A. The predicted boundary of the two domains is indicated by an arrow. Panel B shows the SDS-PAGE analysis of cytochrome c_{550} after limited proteolysis with trypsin and IEX chromatography (Fractogel® EMD TMAE(S)). Lanes: 1– molecular marker; 2– full-length cytochrome c_{550}; 3– protein sample in the column flowthrough assigned to c_{550}[C]; 4– protein sample eluting from the column at 150 mM NaCl assigned to c_{550}[N].
doi:10.1371/journal.pone.0055129.g001

analyzed by SDS-PAGE. As expected, two major products of limited proteolysis were obtained in addition to the band corresponding to non-digested cytochrome (Figure 1B). The bigger fragment in the flowthrough can be attributed to c_{550}[C], while the shorter fragment eluting at 150 mM NaCl likely corresponds to c_{550}[N]. This result confirms that the protein as a whole is strongly dipolar with a negatively charged c_{550}[N] and a positively charged c_{550}[C]. The apparent molecular weights of the proteolytic products ($\sim$7 kDa and $<$7 kDa) are smaller than those predicted for c_{550}[C] and c_{550}[N] (14 kDa and 9 kDa, respectively). This is most likely due to the presence of multiple trypsin cleavage sites within the protein, especially those located at the termini of the domains, more easily accessed by the protease (Figure 1A). The limited proteolysis did not disturb the core of the domains or the heme binding, as the two generated fragments exhibited UV-Vis spectroscopic properties identical to those of the individually expressed domains (see below). This indicates that the two proteolytic fragments correspond to the two domains, each of them being independently folded and associated with one heme cofactor.

The use of recombinantly produced, isolated polypeptidic domains has proven to be a valuable approach to investigate intra- and intermolecular electron transfer between redox centers in multi-domain proteins with largely overlapping spectral properties [30,31]. Therefore, to further confirm the existence of two independent domains in cytochrome c_{550} and to investigate their function, the N- and C-terminal parts of the protein were individually produced in *E. coli*. The recombinant domains contained the PelB signal sequence to promote their translocation to the periplasmic space and fragments of the flexible linker in order to enhance the stability of both domains (Figure 1A). After protein expression and isolation of the periplasmic fractions, the two domains were purified by IEX and size exclusion chromatography (SEC), as described in the Materials and Methods section. The procedure yielded $\sim$95% homogeneous fragments of approximately 9 kDa and 14 kDa corresponding to c_{550}[N] and c_{550}[C], respectively (Figure 2A). The UV-Vis spectra of the reduced c_{550}[N] and c_{550}[C] exhibited a Soret band centered at 415 nm and 417.5 nm, respectively, while c_{550}[C] showed also a composite α band (Figure 2B). This shows that the splitting of the signal does not arise from the presence of two hemes. Instead, it is the result of the transition between the ground state and two or more excited states close in energy. Overall, the spectral properties confirmed that one heme cofactor was successfully incorporated in each domain during recombinant expression in *E. coli*.

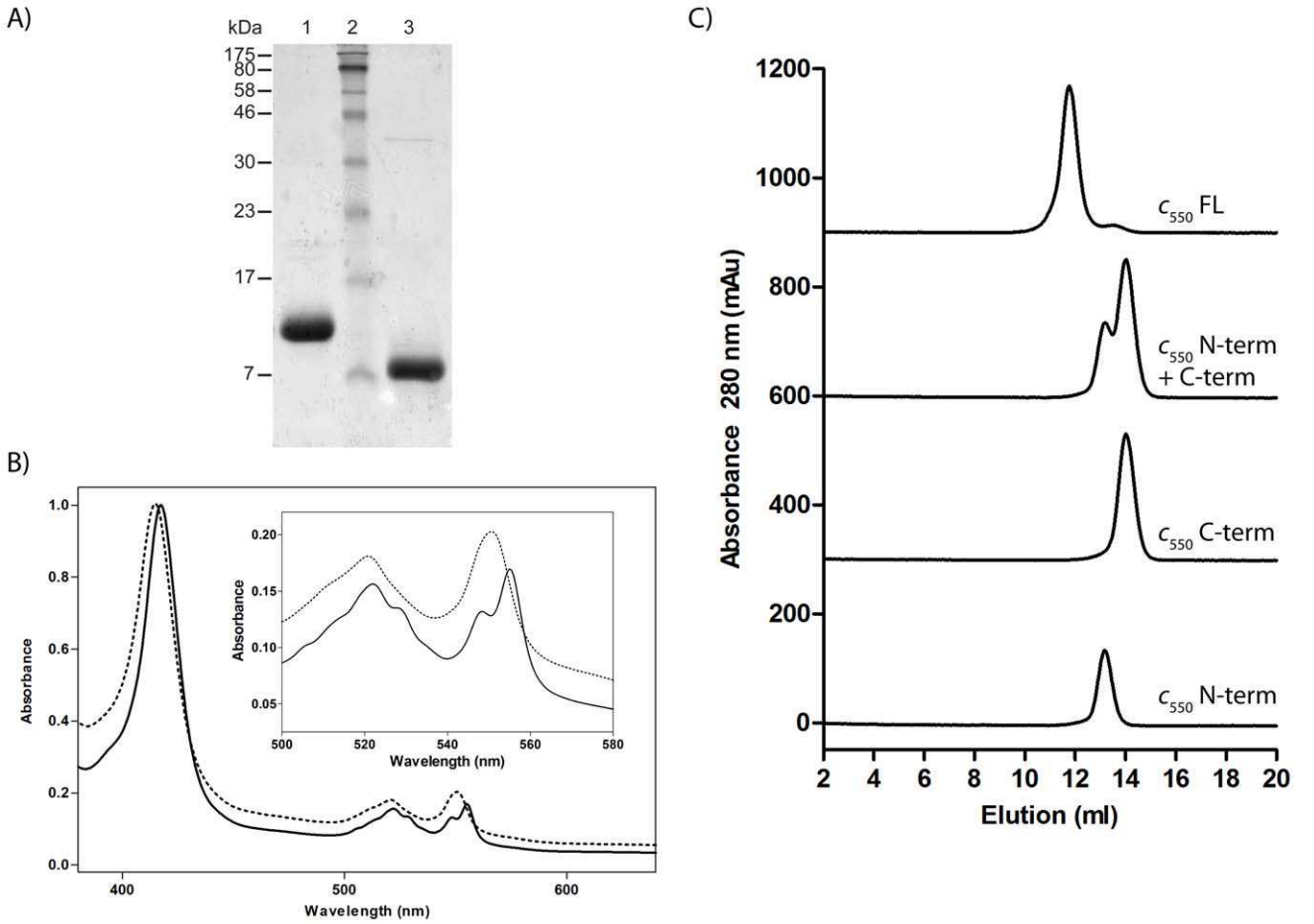

Figure 2. Characterization of the recombinant N- and C-terminal domains of cytochrome c_{550}. The purified domains have been characterized by SDS-PAGE (A), absorption spectroscopy (B) and analytical SEC (C). A. Lanes: 1 and 3– purified c_{550}[C] and c_{550}[N], respectively; 2– molecular marker. B. Absorption spectrum of reduced c_{550}[N] (–) and c_{550}[C] (−). Inset: enlargement of the visible region. C. Analytical SEC chromatograms relative to (from top to bottom) the full-length cytochrome c_{550}, a mixture of c_{550}[C] and c_{550}[N], and each of the two domains analyzed separately.
doi:10.1371/journal.pone.0055129.g002

Separation by IEX chromatography of the domains obtained by limited proteolysis of cytochrome c_{550} (Fig. 1B) argues against the formation of a stable complex between c_{550}[N] and c_{550}[C]. Consistently, when a 1:1 mixture of the two domains was incubated at room temperature for one hour and assayed by analytical SEC, c_{550}[N] and c_{550}[C] eluted separately as individual proteins (Figure 2C). All together the results presented above indicate that cytochrome c_{550} folds into two independent domains with distinct properties, each carrying a single heme group. These features may have implications with regard to the electron transfer activity of the cytochrome.

The N-terminal Domain of Cytochrome c_{550} Accepts the Electrons from SOR_{TTHB8}

We have previously shown that cytochrome c_{550} is the physiological electron acceptor of the sulfite:cytochrome *c* oxidoreductase encoded by the *ttha1326* gene in *T. thermophilus* HB8 [16]. Based on the high similarity between c_{550}[N] and the SorB subunit of the sulfite:cytochrome *c* oxidoreductase from *C. jejuni*, it is very likely that this domain acts as an electron acceptor for SOR_{TTHB8}. The 3D model of SOR_{TTHB8} was automatically built by means of the SWISS-MODEL server [32–34], using as a template the only available structure for a microbial SOR, i.e., the one of the *S. novella* enzyme (PDB ID: 2c9x, segment A; 33% identity to SOR_{TTHB8}) (Figure 3A). In *S. novella* SOR, the formation of complementary electrostatic surfaces at the interface of the SorA and SorB subunit of sulfite:cytochrome *c* oxidoreductase has been observed [35]. Similarly, a positively charged surface area surrounding the pocket cradling the molybdopterin cofactor is present also in the SOR from *T. thermophilus* HB8 (Figure 3A), while the c_{550}[N] presents an overall negative surface charge as shown by IEX chromatography. It is, therefore, reasonable to assume that c_{550}[N] and SOR_{TTHB8} present analogies to typical SORs both in terms of function and type of interactions.

In order to test which domain of cytochrome c_{550} preferably interacts with SOR_{TTHB8}, the electron transfer between the latter enzyme and the recombinant c_{550}[N] or c_{550}[C] was kinetically investigated by stopped-flow spectroscopy. In these experiments, a solution of SOR in the presence of an excess of sulfite was anaerobically mixed at 45°C with increasing amounts of oxidized full-length cytochrome c_{550}, c_{550}[N], c_{550}[C] or a 1:1 mixture of the two domains. As shown in Figure 4A, compared to the full-length protein, c_{550}[C] acts as a very poor electron acceptor for SOR_{TTHB8} even at a final concentration as high as 20 μM (not shown). In contrast, c_{550}[N] is promptly reduced in this

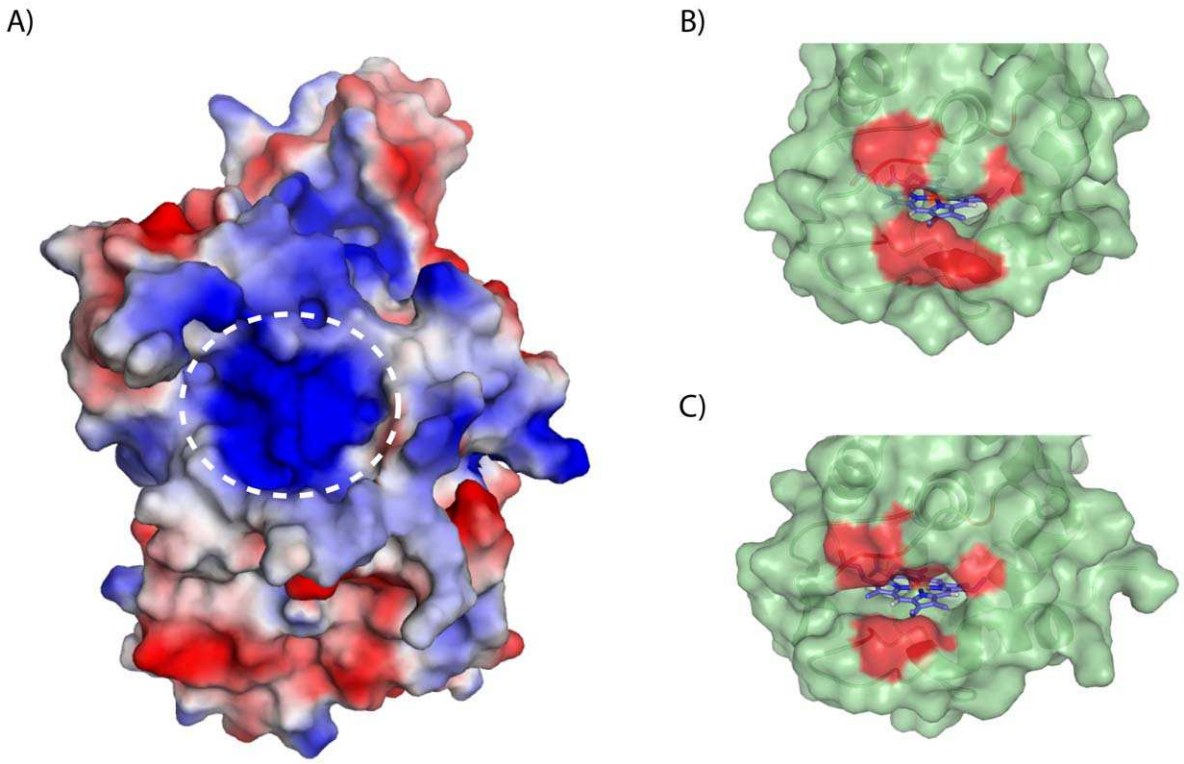

Figure 3. The 3D models of SOR_{TTHB8} (A) and cytochrome c_{550} (B), shown together with the structure of cytochrome c_{552} (PDB ID: 1c52) (C). Structure analysis of SOR_{TTHB8} revealed the positively charged surface area of the protein (A, encircled), believed to be important for interaction with cytochrome c_{550}. The hydrophobic belt surrounding the heme cleft in cytochromes c_{550} (B) and c_{552} (C) is depicted in red.
doi:10.1371/journal.pone.0055129.g003

experimental set up (Figure 4B), which confirms that the N-terminal domain of cytochrome c_{550} is the electron acceptor for SOR_{TTHB8}. Interestingly, a 1:1 mixture of the two cytochrome domains is also completely reduced, although at a slightly lower apparent rate (Figure 4B). This implies that c_{550}[N] and c_{550}[C] are in rapid redox equilibrium and can exchange electrons once reduction of the c_{550}[N] has occurred. Figure 4C reports the average turnover rate of the reaction calculated as detailed in the Materials and Methods and plotted as a function of the concentration of c_{550}[N], either isolated or as part of the full-length protein or mixed in a 1:1 ratio with c_{550}[C]. Under all conditions a linear concentration dependence was observed. Interestingly, c_{550}[N], either isolated or integrated in the full-length protein, is reduced at comparable rates, which further points to the N-terminal domain of cytochrome c_{550} as the electron acceptor for SOR_{TTHB8}.

Electron Transfer from Cytochrome c_{550} to Cytochrome c_{552}

We have previously shown that cytochrome c_{550} passes the electrons generated during sulfite oxidation to the terminal oxidases of the respiratory chain *via* cytochrome c_{552}. To assess which domain of cytochrome c_{550} takes part in this electron transfer, the oxidation of c_{550}[N] or c_{550}[C] by cytochrome c_{552} was tested. The reduced c_{550}[N] or c_{550}[C] were mixed anaerobically with oxidized c_{552} and the reaction was followed at 4°C at ionic strengths ranging from 2 to 152 mM. The reaction was studied under non pseudo-first order conditions and, accordingly, the experimental traces were fitted following the analysis described elsewhere [26]. From the results presented in Figure 5AB it can be concluded that, despite the low temperature, both c_{550}[N] and c_{550}[C] are able to rapidly exchange electrons with cytochrome c_{552}. Table 1 shows the estimated forward (k_F) and reverse (k_R) rate constants of the reaction measured at the same ionic strength (12 mM). The observed differences in k_F and k_R are not significant due to the rather high experimental error in those measurements, partly arising from the large optical overlap among the investigated proteins. Based on the results, we conclude that both c_{550}[N] and c_{550}[C] exchange electrons with cytochrome c_{552} at rates similar to those previously measured with the full-length cytochrome c_{550} [16]. Interestingly, the reaction between c_{550}[N] and c_{552} displays a similar ionic strength dependence to the full-length protein, whereas the dependence is less pronounced in the case of c_{550}[C] (Figure 5C). This suggests that electrostatic forces play an important role in the interaction between c_{550}[N] and c_{552}, while apolar interactions may be involved in molecular recognition between c_{550}[C] and c_{552}.

In order to test this possibility, the 3D model of c_{550}[C] was automatically built by means of the SWISS-MODEL server [32–34], using the X-ray structure of cytochrome c_{552} from *T. thermophilus* HB8 (PDB ID: 1c52; ~50% identity) as template (Figure 3BC). The heme cleft in the very well described cytochrome c_{552} is surrounded by a hydrophobic belt (Figure 3C) consisting of residues G13, C14, F26, V68, M69 and F72; this patch of residues likely participates in the interaction between the cytochrome and the terminal oxidase ba_3 [36]. Interestingly, the model structure of c_{550}[C] clearly shows that such hydrophobic residues (G11, C12, F24, V66, M67 and F70) are structurally conserved around the cleft (Figure 3B). It is therefore likely that molecular recognition between c_{550}[C] and c_{552} is also mediated by this hydrophobic patch, in line with the modest ionic strength dependence reported in Figure 5C.

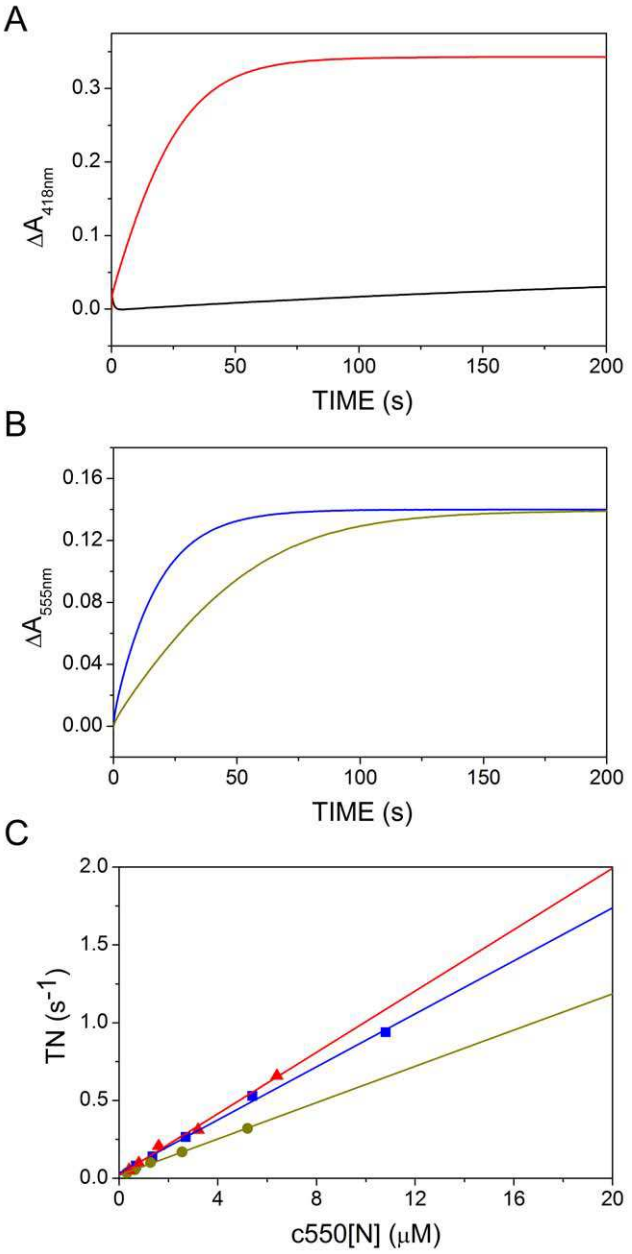

Figure 4. Reduction of cytochrome c_{550} and its domains by SOR_{TTHB8} in the presence of sulfite. In order to reveal the domain of c_{550} accepting electrons from SOR_{TTHB8}, the reduction of full length c_{550} (3.2 μM, red), c_{550}[C] (2.5 μM, black), c_{550}[N] (10.3 μM, blue) or a 1:1 mixture of c_{550}[N] and c_{550}[C] (5.15 μM each, green) by 0.5 μM SOR_{TTHB8} in the presence of 1 mM sulfite was performed (A, B). The experiments were carried out at T = 45°C. Panel C shows the turnover rates (TN) for c_{550} (red), c_{550}[N] (blue) and a mixture of c_{550}[N] and c_{550}[C] (green), calculated as described in Materials and Methods.
doi:10.1371/journal.pone.0055129.g004

Electron Transfer to the Terminal Oxidases caa_3 and ba_3

When assayed separately, c_{550}[N], similarly to full-length c_{550}, is very slowly oxidized by either ba_3 or caa_3 oxidase, whereas c_{550}[C] is quickly oxidized by either of the two oxidases (Figure 6A,B). Considering the high sequence similarity between c_{550}[C] and c_{552} and the structurally conserved hydrophobic belt (Figure 3BC) likely participating in molecular recognition between c_{552} and ba_3-oxidase, this finding is perhaps not unexpected. On the other hand, we have previously shown (and confirmed here) that the electron transfer between full-length c_{550} and ba_3 or caa_3 is not efficient, unless mediated by c_{552} acting as an electron shuttle [16]. Therefore, we suggest that the relatively fast direct electron transfer between c_{550}[C] and terminal oxidases here documented is of no physiological value. If the conserved hydrophobic patch mentioned above is involved in mediating electron transfer from c_{550}[C], in the full-length protein such a patch should be not accessible by large molecules, like ba_3 or caa_3 oxidase, though possibly still allowing interaction with much smaller molecules such as cytochrome c_{552}.

Interestingly, a 1:1 mixture of ascorbate-reduced c_{550}[N] and c_{550}[C] is also quickly and fully oxidized by ba_3 or caa_3 (Figure 6A,B), which further confirms that the two domains of c_{550} are in relatively fast redox equilibrium. Expectedly, in the presence of 10 nM oxidized c_{552}, both c_{550}[N] and c_{550}[C] are promptly oxidized by ba_3 (Figure 6C,D) or caa_3 (data not shown), as previously observed with the full-length protein [16]. This further supports a fast electron transfer between either of the two domains of cytochrome c_{550} and cytochrome c_{552}.

Discussion

While sulfite oxidizing enzymes (SOEs) in vertebrates and humans have been studied for over 40 years, significant progress in studying bacterial SOEs has only been made in the last decade. Bacterial SOEs are extremely diverse in terms of structure and oxidizing proteins. Discovery of novel SOEs is being constantly reported, but in most cases the relative electron acceptor was not identified. Hence, usually the link to the respiratory chain is not shown [12–14,18,20]. The complexity of those pathways is a real challenge for understanding how SOEs participate in cell metabolism and energy production. Recently, the complete sulfite oxidation pathway from *T. thermophilus* has been described [16]; it was shown that the electrons generated during sulfite oxidation are injected into the respiratory chain at the level of cytochromes c_{552}, via the di-heme cytochrome c_{550}. Here we have undertaken a detailed investigation of the role played by the novel cytochrome c_{550} in linking sulfite oxidation to cell respiration.

Sequence analysis, limited proteolysis and individual expression of the N- and C- terminal regions of the cytochrome confirmed that overall the protein consists of two independent domains, each associated with one *c*-type heme. At physiological pH, the protein is most likely characterized by an asymmetric charge distribution: it has a negatively charged N-terminal domain and a positively charged C-terminal one. The detailed analysis of other di-heme *c*-type cytochromes revealed several features shared by c_4-type cytochromes. Cytochromes c_4 are periplasmic or membrane-bound members of class I cytochromes *c* with a molecular mass of ~20 kDa found in a variety of bacteria [37,38]. Analysis of the characterized cytochromes c_4 from *Vibrio cholerae* [39], *Pseudoalteromonas haloplanktis* [40], *Pseudomonas aeruginosa*, *Azotobacter vinelandii* [41], *Acidithiobacillus ferrooxidans* [42] and *Pseudomonas stutzeri* [43,44], and the high resolution X-ray structures of the last two [45,46] show that, similarly to *T. thermophilus* c_{550}, these di-heme proteins are formed by two domains connected with a flexible, ~10 aa long linker.

While *T. thermophilus* c_{550} exhibits only ~15% identity to cytochromes c_4, the latter cytochromes show relatively high sequence similarities not only one each other, but also between the two domains of the same cytochrome (though to a minor extent). This led to the hypothesis that cytochromes c_4 result from duplication of a common ancestral gene [45,46]. Given the low sequence conservation typically observed among multi-heme

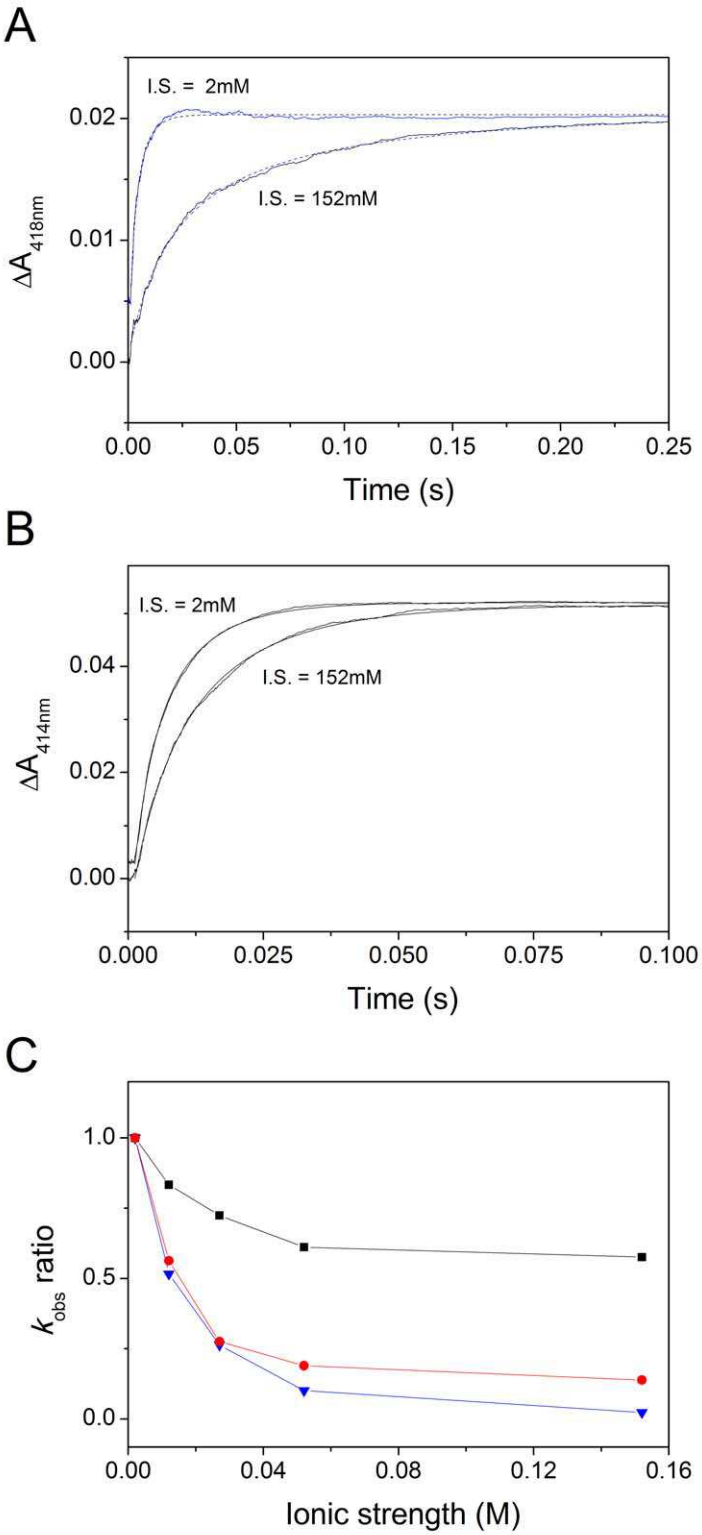

Figure 5. Electron transfer analysis between c_{550}[N], c_{550}[C] and c_{552}. To investigate the electron transfer between c_{550}[N], c_{550}[C] and c_{552}, kinetic traces were collected after anaerobically mixing 3.2 μM ascorbate-reduced c_{550}[N] with 3.2 μM oxidized c_{552} at λ = 418 nm and T = 4°C (A), or mixing 4.1 μM ascorbate-reduced c_{550}[C] with 5.2 μM oxidized c_{552} at λ = 414 nm and T = 4°C (B). Panel C shows the ionic strength dependence of the reaction of c_{550} (red), c_{550}[N] (blue) or c_{550}[C] (black) with c_{552}. Data were normalized for the rate constants measured at ionic strength = 2 mM.
doi:10.1371/journal.pone.0055129.g005

Table 1. Forward (k_F) and reverse (k_R) rate constants estimated at 4°C and at ionic strength = 12 mM for the reaction of cytochrome c_{550} and its domains with cytochrome c_{552}.

	k_F (M^{-1} s^{-1})	k_R (M^{-1} s^{-1})
c_{550}[N]	$\sim 10\times10^7$	$8 \div 30\times10^6$
c_{550}[C]	$\sim 7\times10^7$	$3 \div 7\times10^6$
c_{550}	$\sim 5.5\times10^7$	$5 \div 9\times10^6$

doi:10.1371/journal.pone.0055129.t001

cytochromes *c* [47], it would be tempting to postulate close relationships between *T. thermophilus* c_{550} and cytochromes c_4. In the case of cytochrome c_{550}, however, the fusion of two distantly related cytochromes rather than gene duplication appears to be more likely; the domains indeed exhibit both remarkably different sequences and sizes (with c_{550}[N] and c_{550}[C] representing 1/3 and 2/3 of the full-length protein, respectively). It seems very likely that c_{550}[C] originates from duplication and divergence of cytochrome c_{552} [48]. Similarly, fusion of two distantly related cytochromes has been proposed also for the di-heme cytochrome *c* subunit of the flavocytochrome *c* sulfide dehydrogenase from *Chromatium vinosum*. This subunit exhibits ~15% identity to both cytochromes c_4 [49] and *T. thermophilus* cytochrome c_{550}, while showing a fold very similar to that of cytochrome c_4 [50].

Despite the low sequence similarity, the dipolar nature of *T. thermophilus* cytochrome c_{550} (resulting from an asymmetric charge distribution between the two domains) has been also reported for the cytochromes c_4 isolated from *P. stutzeri* and *A. ferrooxidans* [43,45,46]. It has been proposed that the dipolar nature of the cytochrome c_4 from *P. stutzeri* is important for the interaction of the cytochrome with its redox partners. The positively charged C-terminal domain is proposed to interact with the negatively charged pocket of cytochrome *c* oxidase, while negatively charged N-terminal domain with a reductase [45]. However, despite the extensive characterization of *P. stutzeri* cytochrome c_4 (see references in [44]), its specific physiological function remains to be established as yet. Conversely, analysis of the cytochrome c_4 from *A. ferrooxidans* showed the crucial role of a negatively charged residue E121 localized on the overall positively charged C-terminal domain in recognition of its electron donor, rusticyanin, while the Y63 localized in the negatively charged N-terminal domain seems to be responsible for the electron transfer from c_4 to cytochrome *c* oxidase [51].

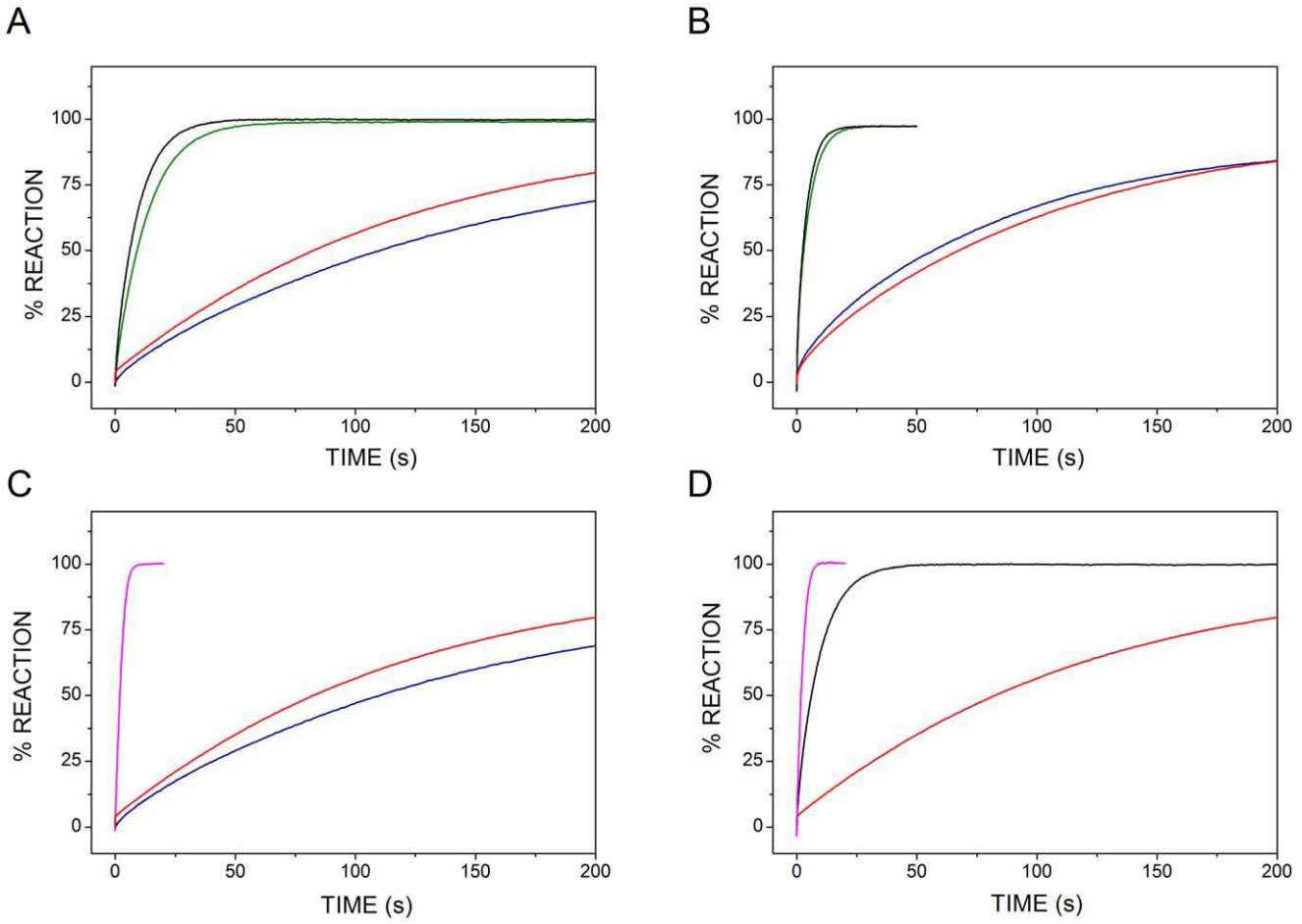

Figure 6. Electron transfer between the domains of c_{550} and terminal oxidases ba_3 and caa_3 in the absence (A,B) or in the presence (C, D) of cytochrome c_{552}. Oxidation by ba_3 (A) or caa_3 (B) oxidase of ascorbate-reduced c_{550} (red), c_{550}[C] (black), c_{550}[N] (blue) or a 1:1 mixture of the two domain (green). In C and D, the oxidation of c_{550}[N] or c_{550}[C] by ba_3 oxidase was investigated in the presence of 10 nM c_{552} (magenta). T = 25°C.

doi:10.1371/journal.pone.0055129.g006

The results presented here clearly show that the N- (but not the C-) terminal domain of *T. thermophilus* cytochrome c_{550} binds to and accepts electrons from SOR_{TTHB8}. Based on the 3D model generated for SOR_{TTHB8} and IEX chromatography experiments on c_{550}[N], recognition between these two proteins most likely involves electrostatic interactions between the positively charged area surrounding the molybdopterin cofactor in SOR_{TTHB8} and the overall negative charge of c_{550}[N]. Electrostatic interactions have been also proposed to drive the reaction of SorT from *S. meliloti* with its negatively charged natural electron acceptor, cytochrome Smc04048 [20]. The importance of electrostatic interactions between SOR_{TTHB8} and c_{550}[N] is further supported by the presence of a conserved arginine residue (R50) in the SOR_{TTHB8} in a position that has been identified as crucial for electron transfer in SorA from *S. novella* (R55) [35,52]. Functionally, therefore, the c_{550}[N] resembles the heme subunit of a classical Group 1 SOR, and the full-length cytochrome c_{550} resembles the cytochrome *c* subunit of the flavocytochrome *c* sulfide dehydrogenase from *Chromatium vinosum*, where the N-terminal part of the di-heme cytochrome *c* tightly interacts with the flavin-containing enzymatically active subunit of the protein.

Our results show that the two domains of cytochrome c_{550} can rapidly exchange electrons once the c_{550}[N] has been reduced by SOR_{TTHB8}. Furthermore, both domains are also able to reduce cytochrome c_{552}, the molecule connecting sulfite oxidation directly to the respiratory chain. The c_{550}[C] most likely binds c_{552} *via* hydrophobic interactions and electron transfer is therefore only modestly affected by the ionic strength. Hydrophobic interactions have also been proposed to be involved in the reaction of cytochrome c_4 from *A. ferrooxidans* [46,51] with its electron acceptor. Moreover they have also been shown to be particularly important in *T. thermophilus* [30] and in thermophilic organisms in general, as electrostatic interactions are weakened at high temperatures [53].

The finding that both domains of *T. thermophilus* c_{550} can pass electrons to c_{552} rules out the possibility that the protein acts as a wire, where one heme serves as the entrance and the other as the exit site for electrons. Our results show that in principle the pathway could be functional with only c_{550}[N], as this domain is able by itself to shuttle electrons from SOR_{TTHB8} to c_{552}. The c_{550}[C] seems, therefore, dispensable for c_{550} to fulfill its function. However, the presence of a second heme center in rapid redox equilibrium with both c_{550}[N] and c_{552} enables cytochrome c_{550} to assist a two-electron transfer process, similarly to the di-heme subunit of flavocytochrome *c* sulfide dehydrogenase from *C. vinosum* [50]. This confers to cytochrome c_{550} the ability to store the two electrons generated during oxidation of a single sulfite molecule and inject them into the terminal oxidases of the respiratory chain *via* cytochrome c_{552}, thereof ensuring an efficient coupling between sulfite oxidation and the respiration-mediated energy production.

Acknowledgments

We thank T. Palmer for the *E. coli* TP1000 strain and L. Thöny-Meyer for the plasmid pEC86.

Author Contributions

Conceived and designed the experiments: SR AG TS MA EF PS. Performed the experiments: SR MA EF PS. Analyzed the data: SR OKR AG TS MA EF PS. Contributed reagents/materials/analysis tools: SR OKR AG TS MA EF PS. Wrote the paper: SR OKR.

References

1. Griffith OW (1987) Mammalian sulfur amino acid metabolism: an overview. Methods Enzymol 143: 366–376.
2. Kappler U, Dahl C (2001) Enzymology and molecular biology of prokaryotic sulfite oxidation. FEMS Microbiol Lett 203: 1–9.
3. Cook AM, Denger K (2006) Metabolism of taurine in microorganisms: a primer in molecular biodiversity? Adv Exp Med Biol 583: 3–13.
4. Brune DC (1995) Sulfur compounds as photosynthetic electron donors. In: Blankenship RE, Madigan MT, Bauer CE, editors. Anoxygenic photosythetic bacteria. Dordrecht: Kluwer Academic Publishers. 847–870.
5. Sorokin DY (1995) *Sulfitobacter pontiacus* gen. nov., sp. nov. - a new heterotrophic bacterium from the Black Sea, specialized on sulfite oxidation. Microbiology (English translation of Mikrobiologiia) 64: 295–305.
6. Feng C, Tollin G, Enemark JH (2007) Sulfite oxidizing enzymes. Biochim Biophys Acta 1774: 527–539.
7. Cohen HJ, Fridovich I (1971) Hepatic sulfite oxidase. The nature and function of the heme prosthetic groups. J Biol Chem 246: 367–373.
8. Kessler DL, Rajagopalan KV (1972) Purification and properties of sulfite oxidase from chicken liver. Presence of molybdenum in sulfite oxidase from diverse sources. J Biol Chem 247: 6566–6573.
9. Eilers T, Schwarz G, Brinkmann H, Witt C, Richter T, et al. (2001) Identification and biochemical characterization of *Arabidopsis thaliana* sulfite oxidase. A new player in plant sulfur metabolism. J Biol Chem 276: 46989–46994.
10. Kappler U, Bennett B, Rethmeier J, Schwarz G, Deutzmann R, et al. (2000) Sulfite:Cytochrome *c* oxidoreductase from *Thiobacillus novellus*. Purification, characterization, and molecular biology of a heterodimeric member of the sulfite oxidase family. J Biol Chem 275: 13202–13212.
11. Charles AM, Suzuki I (1965) Sulfite oxidase of a facultative autotroph, *Thiobacillus novellus*. Biochem Biophys Res Commun 19: 686–690.
12. Denger K, Weinitschke S, Smits TH, Schleheck D, Cook AM (2008) Bacterial sulfite dehydrogenases in organotrophic metabolism: separation and identification in *Cupriavidus necator* H16 and in *Delftia acidovorans* SPH-1. Microbiology 154: 256–263.
13. D'Errico G, Di Salle A, La Cara F, Rossi M, Cannio R (2006) Identification and characterization of a novel bacterial sulfite oxidase with no heme binding domain from *Deinococcus radiodurans*. J Bacteriol 188: 694–701.
14. Di Salle A, D'Errico G, La Cara F, Cannio R, Rossi M (2006) A novel thermostable sulfite oxidase from *Thermus thermophilus*: characterization of the enzyme, gene cloning and expression in *Escherichia coli*. Extremophiles 10: 587–598.
15. Wilson JJ, Kappler U (2009) Sulfite oxidation in *Sinorhizobium meliloti*. Biochim Biophys Acta 1787: 1516–1525.
16. Robin S, Arese M, Forte E, Sarti P, Giuffre A, et al. (2011) A sulfite respiration pathway from *Thermus thermophilus* and the key role of newly identified cytochrome c_{550}. J Bacteriol 193: 3988–3997.
17. Reichenbecher W, Kelly DP, Murrell JC (1999) Desulfonation of propanesulfonic acid by *Comamonas acidovorans* strain P53: evidence for an alkanesulfonate sulfonatase and an atypical sulfite dehydrogenase. Arch Microbiol 172: 387–392.
18. Myers JD, Kelly DJ (2005) A sulphite respiration system in the chemoheterotrophic human pathogen *Campylobacter jejuni*. Microbiology 151: 233–242.
19. Kappler U (2011) Bacterial sulfite-oxidizing enzymes. Biochim Biophys Acta 1807: 1–10.
20. Low L, Kilmartin JR, Bernhardt PV, Kappler U (2011) How are "Atypical" Sulfite Dehydrogenases Linked to Cell Metabolism? Interactions between the SorT Sulfite Dehydrogenase and Small Redox Proteins. Front Microbiol 2: 58.
21. Soulimane T, Kiefersauer R, Than ME (2002) ba_3-cytochrome *c* oxidase from *Thermus thermophilus*: purification, crystallisation and crystal transformation. A Practical Guide to Membrane Protein Purification and Crystallization: Academic Press. 229–251.
22. Gerscher S, Hildebrandt P, Soulimane T, Buse G (1998) Resonance Raman spectroscopic study of the caa_3 oxidase from *Thermus thermophilus*. Biospectroscopy 4: 365–377.
23. Soulimane T, von Walter M, Hof P, Than ME, Huber R, et al. (1997) Cytochrome c_{552} from *Thermus thermophilus*: a functional and crystallographic investigation. Biochem Biophys Res Commun 237: 572–576.
24. Arslan E, Schulz H, Zufferey R, Kunzler P, Thony-Meyer L (1998) Overproduction of the *Bradyrhizobium japonicum c*-type cytochrome subunits of the cbb_3 oxidase in *Escherichia coli*. Biochem Biophys Res Commun 251: 744–747.
25. Higuchi M, Hirano Y, Kimura Y, Oh-oka H, Miki K, et al. (2009) Overexpression, characterization, and crystallization of the functional domain of cytochrome *c*(z) from *Chlorobium tepidum*. Photosynth Res 102: 77–84.
26. Malatesta F (2005) The study of bimolecular reactions under non-pseudo-first order conditions. Biophys Chem 116: 251–256.
27. Marsden RL, McGuffin LJ, Jones DT (2002) Rapid protein domain assignment from amino acid sequence using predicted secondary structure. Protein Science 11: 2814–2824.
28. George RA, Heringa J (2002) An analysis of protein domain linkers: their classification and role in protein folding. Protein Eng 15: 871–879.
29. Royer CA (2006) Probing protein folding and conformational transitions with fluorescence. Chem Rev 106: 1769–1784.

30. Janzon J, Ludwig B, Malatesta F (2007) Electron transfer kinetics of soluble fragments indicate a direct interaction between complex III and the *caa*$_3$ oxidase in *Thermus thermophilus*. IUBMB Life 59: 563–569.
31. Mooser D, Maneg O, Corvey C, Steiner T, Malatesta F, et al. (2005) A four-subunit cytochrome *bc*(1) complex complements the respiratory chain of *Thermus thermophilus*. Biochim Biophys Acta 1708: 262–274.
32. Arnold K, Bordoli L, Kopp J, Schwede T (2006) The SWISS-MODEL workspace: a web-based environment for protein structure homology modelling. Bioinformatics 22: 195–201.
33. Guex N, Peitsch MC (1997) SWISS-MODEL and the Swiss-Pdb Viewer: An environment for comparative protein modeling. ELECTROPHORESIS 18: 2714–2723.
34. Schwede T, Kopp J, Guex N, Peitsch MC (2003) SWISS-MODEL: an automated protein homology-modeling server. Nucleic Acids Research 31: 3381–3385.
35. Kappler U, Bailey S (2005) Molecular basis of intramolecular electron transfer in sulfite-oxidizing enzymes is revealed by high resolution structure of a heterodimeric complex of the catalytic molybdopterin subunit and a c-type cytochrome subunit. J Biol Chem 280: 24999–25007.
36. Giuffre A, Forte E, Antonini G, D'Itri E, Brunori M, et al. (1999) Kinetic properties of *ba*$_3$ oxidase from *Thermus thermophilus*: effect of temperature. Biochemistry 38: 1057–1065.
37. Pettigrew GW, Moore GR (1987) Cytochromes c - Biological aspects. Berlin Heidelberg: Springer-Verlag.
38. Moore GR, Pettigrew GW (1990) Cytochromes *c* - Evolutionary, structural and physicochemical aspects. Berlin Heidelberg: Springer-Verlag.
39. Chang HY, Ahn Y, Pace LA, Lin MT, Lin YH, et al. (2010) The diheme cytochrome c_4 from *Vibrio cholerae* is a natural electron donor to the respiratory *cbb*$_3$ oxygen reductase. Biochemistry 49: 7494–7503.
40. Di Rocco G, Battistuzzi G, Borsari M, De Rienzo F, Ranieri A, et al. (2008) Cloning, expression and physicochemical characterization of a di-heme cytochrome c (4) from the psychrophilic bacterium *Pseudoalteromonas haloplanktis* TAC 125. J Biol Inorg Chem 13: 789–799.
41. Pettigrew GW, Brown KR (1988) Free and membrane-bound forms of bacterial cytochrome c4. Biochem J 252: 427–435.
42. Giudici-Orticoni MT, Leroy G, Nitschke W, Bruschi M (2000) Characterization of a new dihemic c(4)-type cytochrome isolated from *Thiobacillus ferrooxidans*. Biochemistry 39: 7205–7211.
43. Conrad LS, Karlsson JJ, Ulstrup J (1995) Electron transfer and spectral alpha-band properties of the di-heme protein cytochrome c4 from *Pseudomonas stutzeri*. Eur J Biochem 231: 133–141.
44. Raffalt AC, Schmidt L, Christensen HE, Chi Q, Ulstrup J (2009) Electron transfer patterns of the di-heme protein cytochrome c(4) from *Pseudomonas stutzeri*. J Inorg Biochem 103: 717–722.
45. Kadziola A, Larsen S (1997) Crystal structure of the dihaem cytochrome c4 from *Pseudomonas stutzeri* determined at 2.2A resolution. Structure 5: 203–216.
46. Abergel C, Nitschke W, Malarte G, Bruschi M, Claverie JM, et al. (2003) The structure of *Acidithiobacillus ferrooxidans* c(4)-cytochrome: a model for complex-induced electron transfer tuning. Structure 11: 547–555.
47. Heitmann D, Einsle O (2005) Structural and biochemical characterization of DHC2, a novel diheme cytochrome *c* from *Geobacter sulfurreducens*. Biochemistry 44: 12411–12419.
48. Chothia C, Gough J, Vogel C, Teichmann SA (2003) Evolution of the Protein Repertoire. Science 300: 1701–1703.
49. Van Beeumen JJ, Demol H, Samyn B, Bartsch RG, Meyer TE, et al. (1991) Covalent structure of the diheme cytochrome subunit and amino-terminal sequence of the flavoprotein subunit of flavocytochrome *c* from *Chromatium vinosum*. J Biol Chem 266: 12921–12931.
50. Chen ZW, Koh M, Van Driessche G, Van Beeumen JJ, Bartsch RG, et al. (1994) The structure of flavocytochrome *c* sulfide dehydrogenase from a purple phototrophic bacterium. Science 266: 430–432.
51. Malarte G, Leroy G, Lojou E, Abergel C, Bruschi M, et al. (2005) Insight into molecular stability and physiological properties of the diheme cytochrome CYC41 from the acidophilic bacterium *Acidithiobacillus ferrooxidans*. Biochemistry 44: 6471–6481.
52. Emesh S, Rapson TD, Rajapakshe A, Kappler U, Bernhardt PV, et al. (2009) Intramolecular electron transfer in sulfite-oxidizing enzymes: elucidating the role of a conserved active site arginine. Biochemistry 48: 2156–2163.
53. Maneg O, Malatesta F, Ludwig B, Drosou V (2004) Interaction of cytochrome *c* with cytochrome oxidase: two different docking scenarios. Biochim Biophys Acta 1655: 274–281.